THE LEVELS OF ^{91}Nb POPULATED BY (α, 2n) REACTION

By A. Bałanda, R. Kulessa, W. Waluś

Institute of Physics, Jagellonian University, Cracow*

and J. Sieniawski

Institute of Nuclear Physics, Cracow

(Received July 31, 1975)

The reaction (α, 2nγ) on the ^{89}Y target was used to populate excited states in ^{91}Nb. The gamma-ray transitions belonging to this nucleus were identified by studying excitation functions and gamma-gamma coincidences. Angular distributions, life-time measurements and coincidences with charged particles were also performed. The shell model analysis is used to interpret the observed levels. Nearly all levels belonging to the $(g_{9/2})^3$ and $p_{1/2}(g_{9/2})^2$ proton configurations were found. Matrix elements of the effective proton-proton interactions were determined from the positions of the negative-parity states. These were used to calculate the energy differences of the positive parity states. Satisfactory agreement between the theoretical and experimental values was obtained.

1. Introduction

The level scheme of ^{91}Nb has been recently studied using the stripping reactions [1], (p, γ) [2], (p, n) [3], (α, p2n) [4], (α, 2n) [5] and ^{6}Li induced reactions [6]. A theoretical description of ^{91}Nb, basing on the shell model, has been presented in [7–9]. Most of the experimental data agree with predictions of the model in which ^{88}Sr is an inert core and 3 protons are placed on $2p_{1/2}$ and $1g_{9/2}$ single particle levels. However, all existing sets of the two-body matrix elements cannot explain correctly the succession of levels belonging to the $(g_{9/2})^3$ as well as to the $p_{1/2}$ $(g_{9/2})^2$ configurations. A common feature of the mentioned theoretical calculations [7–9] is the application of the two-body matrix elements, as parameters to the fit of the experimental data taken from nuclei of the region in question. The reason for this is the fact that, for any individual nucleus, good and complete experimental data are lacking. Stripping and pick-up reactions, because of their selectivity excite only some of the energy levels. On the other hand, heavy ion-induced reactions populate preferentially high-spin and yrast levels.

* Address: Instytut Fizyki UJ, Reymonta 4, 30-059 Kraków, Poland.

In our experiment, alpha particle-induced reactions were used to populate the excited states in ^{91}Nb. The complete set of negative parity levels belonging to the $p_{1/2}\,(g_{9/2})^2$ configurations was found. From the energy splitting of the negative parity states, the differences of the two-body matrix elements $V_k - V_0$ (with $k = 2, 4, 6, 8$) were calculated. Using the obtained differences between matrix elements, the energy levels belonging to the $(g_{9/2})^3$ configuration were evaluated. The agreement with experimental data is quite good.

2. *Experimental*

2.1. Target, reactions and instrumentation

The excited states of ^{91}Nb were populated using the reaction $(\alpha, 2n\gamma)$. A metallic Y foil target of about 10 mg/cm^2 thickness was used. In some measurements, 2 and 20 mg/cm^2 targets were used. The measurements were performed using the C–120 cyclotron of the Institute of Nuclear Physics in Cracow. The beam size at the target was usually 5 mm and the beam current about 3 nA or less. The cyclotron beam was bunched with a repetition time of about 100 nsec. The gamma-rays due to the reaction were detected by 16 cm^3 coaxial (FWHM 3 keV at 1173 keV) and 2.2 cm^3 planar (FWHM 1.8 keV at 122 keV) Ge(Li) detectors. For coincidence measurements, NaJ(Tl)–Ge(Li) and Ge(Li)–Ge(Li) detectors and standard ORTEC equipment were used. The data analysis was performed on the ODRA 1204 computer at the Institute of Physics of the Jagiellonian University.

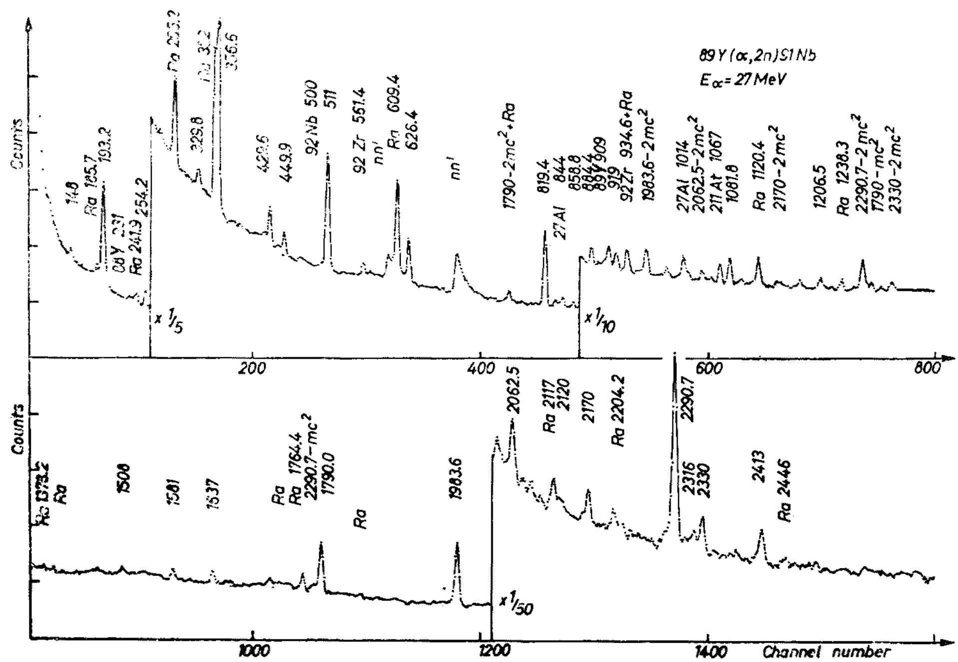

Fig. 1. Gamma-ray spectrum obtained from the ^{89}Y$(\alpha, 2n\gamma)$ ^{91}Nb reaction at 26 MeV. The ^{226}Ra source was placed near the target for calibration

2.2. Measurements of E_γ, I_γ, $I_\gamma(E)$ and $\gamma-\gamma$ coincidences

A typical single gamma-ray spectrum is shown in Fig. 1. For the energy determination, spectra were collected at the angle 90°, relative to the beam direction. For gamma-ray intensity measurements, the detector was placed at about 126°. Aluminium absorbers were used to degrade the alpha-particle energy to below 20 MeV. This allowed us to identify lines belonging to ^{92}Nb (due to the (α, n) reaction). Excitation functions for gamma-rays were measured in the energy range 24.6 MeV to 27.8 MeV. The results for the strongest gamma-rays are shown in Fig. 2. Results are normalized to $I_\gamma/I_{1082} = 1$ for the highest energy of α particles. Such a representation of the excitation function is sometimes very useful for the determination of the position of the level from which the transition begins. For example, the shapes of excitation functions for 193.2 keV and 1983.6 keV lines are the same, which can be explained by the fact that both lines deexcite the same level. If for a sequence of levels with increasing energies their respective spin values also increase, such representation is also convenient to estimate the relative spin values. The

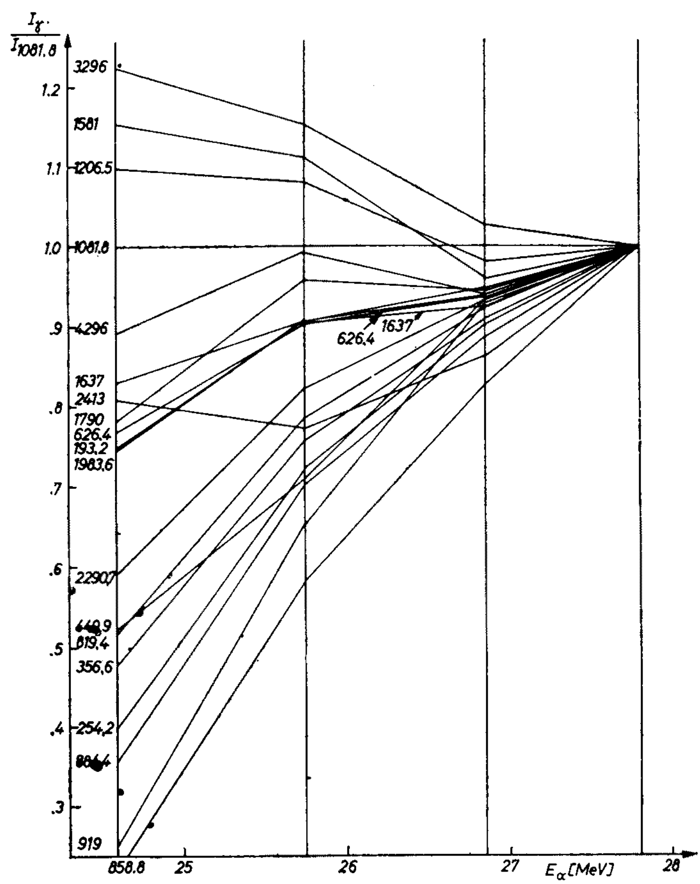

Fig. 2. Excitation function of gamma-rays assigned to ^{91}Nb

TABLE I

Gamma-gamma coincidences in ^{91}Nb

Coincident γ-rays [keV]	NaJ (Tl) gate [keV]					Ge(Li) gate [keV]	
	150–180	180–210	320–390	1900–2100	2200–2400	2290	2330
109						weak	yes
122						yes	
148					weak	yes	weak
193.2						yes	
254.2				yes	yes		
356.9	weak				yes	yes	
429.6				yes			
626.4				weak			
819.4			yes		yes	yes	
858.8					weak	weak	
884.4	weak		yes		yes	yes	
919				yes			
1790.0	weak	yes					
2062.5				weak			
2290.7	yes	weak	yes				

cascade of 356.9, 819.4 and 2290.2 keV lines between $21/2^+$, $17/2^+$, $13/2^+$ and $9/2^+$ states is a good example for use of excitation functions.

Gamma-gamma coincidence measurements were carried out at $E_\alpha = 26$ MeV. Energy gates for the NaJ(Tl) detector were set at ranges 150–180, 180–210, 320–390, 1900–2100 and 2200–2400 keV. When the Ge(Li) detector was used, the gates were placed over the range of full energy peaks at 2290 and 2330 keV and the neighbouring background portions of these photopeaks. The results of these measurements are summarized in Table I.

The residual gamma-ray activity of the target was investigated. From such measurements one can see that alpha particles with energy 26 MeV produce ^{92}Nb and ^{88}Y (1836 and 898 keV transitions) in addition to ^{91}Nb.

Gamma-particle coincidence measurements were also performed. Strong lines (934 and 560 keV) belonging to ^{92}Zr from (α, pγ) reaction were observed. These lines in our single spectrum are rather weak.

2.3. Angular distributions of gamma-rays

The gamma-ray angular distributions aid in finding the spin assignment of the excited states. Tables for calculating angular distributions of gamma-rays have been published by Yamazaki [10]. A new way of calculating the attenuation coefficients for gamma-rays from yrast levels produced by the (α, xn) reaction, has been given by Ejiri et al. [11].

The experimental function of the angular distribution of gamma-rays can be expressed as

$$W(\theta) = 1 + A_2^{max}\alpha_2 P_2(\cos\theta) + A_4^{max}\alpha_4 P_4(\cos\theta) \qquad (1)$$

where α_k are attenuation coefficients. The gamma-ray angular distributions were measured at $E_\alpha = 24.7$ MeV in seven positions, within $-30°$ and $+120°$, relative to the beam direction. The ^{89}Y target used in this experiment was thick and the wall of the target chamber was covered with a thin lead sheet. In such conditions one can measure the intensity of gamma-rays at 0° to the beam direction. This point is very important for accurate measurements of the A_k coefficients.

TABLE II

Gamma-ray transitions used for the determination of the α_2

E_γ[keV]	I_γ/I_{2290}[%]	$J_i \to J_f$	A_2^{exp}	A_4^{exp}	A_2^{max}	α_2
356.6	73.7	21/2⁺ → 17/2⁺	0.32±0.03	−0.10±0.04	0.408	0.78±0.07
819.4	77.2	17/2⁺ → 13/2⁺	0.30±0.03	−0.06±0.04	0.420	0.71±0.07
2290.7	100.0	13/2⁺ → 9/2⁺	0.29±0.03	−0.05±0.03	0.440	0.66±0.07
1790.0	78.0	9/2⁻ → 9/2⁺	0.28±0.02	0.02±0.03	0.485	0.57±0.04
1081.8	11.5	5/2⁻ → 1/2⁻	0.23±0.03	−0.03±0.03	0.571	0.40±0.05

TABLE III

Gamma-ray transitions from the reaction ^{89}Y(α, 2n) ^{91}Nb (see also Table II)

E_γ[keV]	I_γ/I_{2290}[%]	A_2^{exp}	A_4^{exp}	Assignment	
50	8*				17/2⁻ → 13/2⁻
109	4				
122	2				
148	8				
193.2	70	0.27±0.03	−0.04±0.04	E2	13/2⁻ → 9/2⁻
254.2	15	−0.32±0.09	0.01±0.05	dipole	
329.8	3				
429.6	11	0.34±0.03	0.01±0.03	M1+E2	11/2⁻ → 13/2⁻
449.9	7	−0.34±0.08	0.07±0.08	E1	17/2⁺ → 15/2⁻
626.4	19	−0.06±0.03	−0.02±0.03	M1	15/2⁻ → 17/2⁻
858.8	6	−0.63±0.33	0.26±0.50	dipole	
884.4	10	0.28±0.11	0.12±0.12		
919	8	−0.76±0.14	0.08±0.13	E1+M2	(15/2⁺) → 13/2⁻
1206.5	8				
1508	3				
1581	8	−0.38±0.06	0.03±0.05	(M1)+E2	7/2⁺ → 9/2⁺
1637	11	−0.10±0.06	−0.06±0.06	(M1+E2)	9/2⁺ → 9/2⁺
1983.6	92	0.12±0.03	−0.03±0.04	M2+E3	13/2⁻ → 9/2⁻
2062.5	15				
2120	10				
2170	16	0.23±0.04	0.10±0.05	dipole	11/2 → 9/2⁺
2316	4				
2330	14	−0.09±0.03	0.23±0.05	(M1)+E2	(11/2⁺) → 9/2⁺
2413	15	−0.18±0.05	−0.04±0.06	E1	11/2⁻ → 9/2⁺

* Conversion coefficient is equal to about 13.

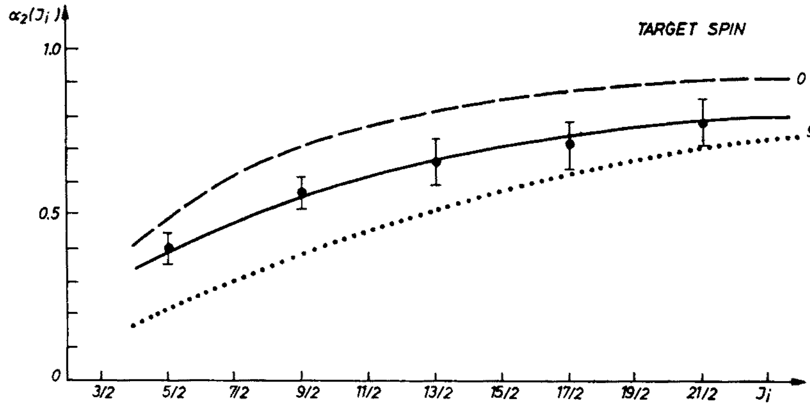

Fig. 3. Attenuation coefficients α_2 obtained from the angular distribution of gamma-rays following the $^{89}Y(\alpha, 2n\gamma)\,^{91}Nb$ reaction. The dashed curves present the calculated [12] dependence for target spin equal to 0 and 9/2. The solid curve denotes values which were used for the analysis of other experimental data

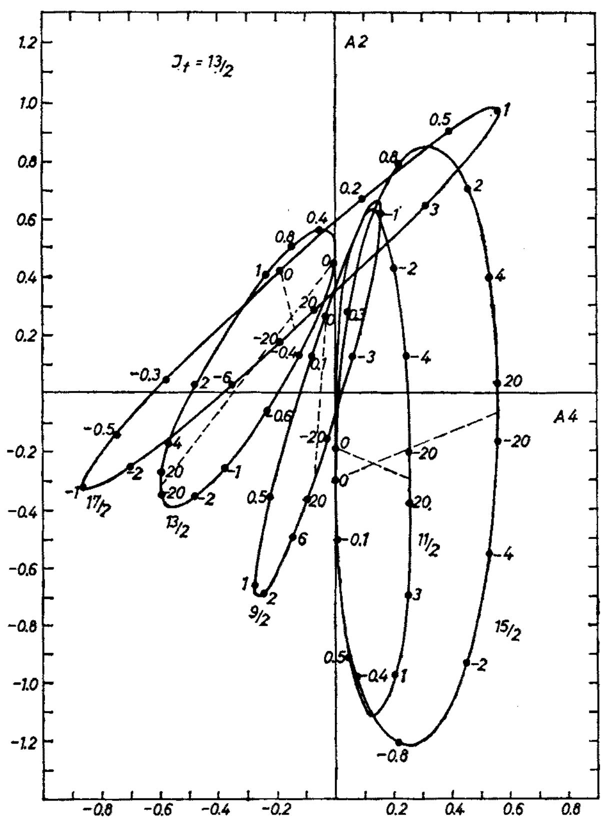

Fig. 4. Example of parametrical representation of A_2^{max} and A_4^{max} for the final spin $J_f = 13/2$

Among many transitions belonging to the ^{91}Nb there are a few for which the multipolarities are well known [4]. One can use these for the experimental determination of the attenuation coefficients, α_k. In Table II experimental results are presented for five transitions which were used for the determination of the α_2 coefficients. The α_2 values, together with the calculated curves [12], are given in Fig. 3.

Theoretical values of $A_2^{\max}$ and $A_4^{\max}$ which are the angular distribution coefficients of gamma-rays emitted from the state with completely aligned spin, were calculated according to the Yamazaki formalism [10]. The parametrical representation of the results of these calculations is given in Fig. 4. Taking the α_2 value from Fig. 3 and assuming the dependence $\alpha_4 = f(\alpha_2)$ [10] one can evaluate $A_2^{\max}$ and $A_4^{\max}$ for any measured transition. A full list of the strongest observed transitions with suggested spin values is presented in Table III.

2.4. Life-time measurements

The literature data concerning the life-time measurements of excited states of ^{91}Nb are not consistent. Baba et al. [5] give for the 17/2$^-$ (2378 keV — probably does not exist) state of ^{91}Nb the value $\tau = (14.4 \pm 0.5)$ nsec and $g = 1.25 \pm 0.04$. In a later paper by Brown et al. [6] one finds for this level (2035 keV) the value (5.42 ± 0.18) μsec. To solve this ambiguity, we have carried out life-time measurements for the 1983.4 keV 13/2$^-$ state.

A typical coincidence setup using ORTEC electronics was applied. Coincidences between Ge(Li) gamma-ray detector pulses and α-beam bursts were measured. Two time-

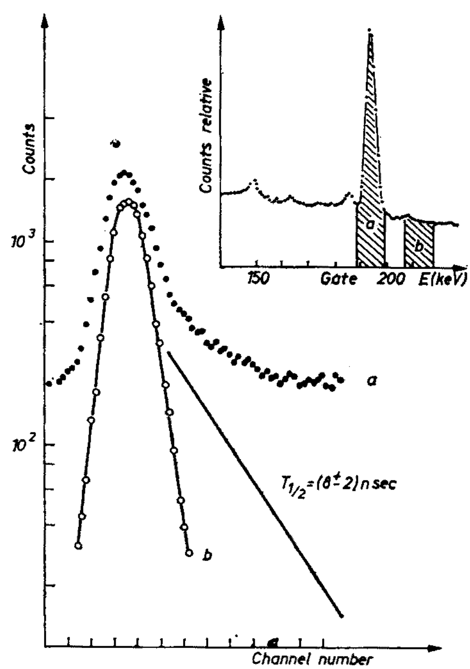

Fig. 5. Life-time measurements of the 1983.4 keV 13/2$^-$ state of ^{91}Nb. For explanation, see text

spectra were collected simultaneously. For the first spectrum, fast pulses were gated by the 193.2 keV photopeak (Fig. 5, *a*), while for the second spectrum the gate was placed over the neighbouring background portions of this peak (Fig. 5, *b*). After subtracting a constant value from curve *a*, one obtains the value of $T_{1/2} = (8 \pm 2)$ nsec. This constant value can correspond to the long-living fraction of this peak, which may follow from the fact that the 13/2⁻ level is fed mainly from the 17/2⁻ long-living state (50 keV transition).

Quite clear Doppler effect for 2413, 2330, 2120 and 1206.5 keV lines in single gamma-ray spectra was observed, so the corresponding levels in ^{91}Nb must deexcite in time shorter than 1 psec.

3. *Energy levels of ^{91}Nb*

The level scheme for ^{91}Nb is presented in Fig. 6. This scheme contains some levels which were observed only in (α, 2nγ) reaction, and was constructed using mainly our results. We have also been guided by results of other authors [2, 4, 6].

The levels at 2290.7, 3110 and 3467 keV have been observed earlier by Grecescu et al.

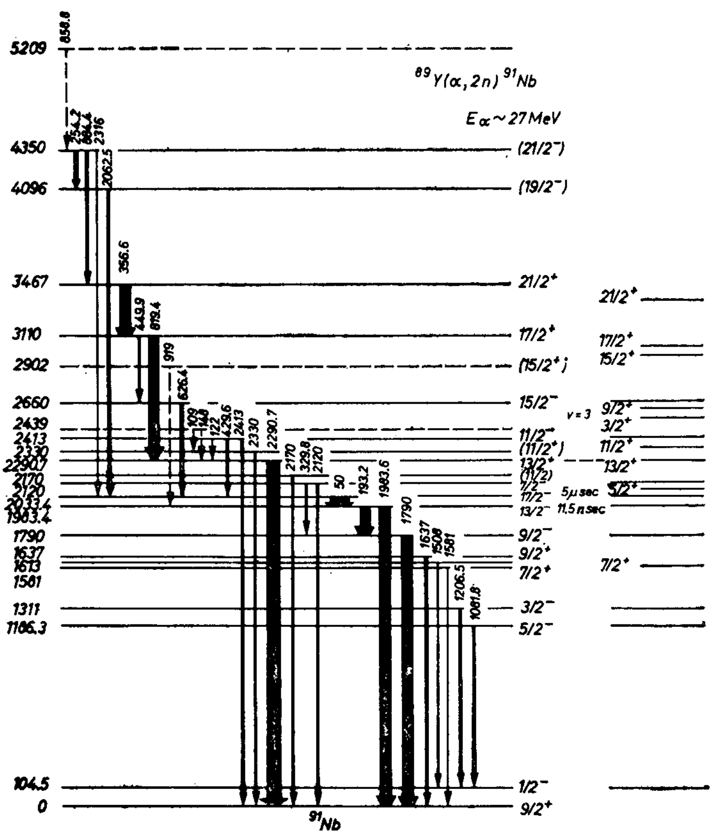

Fig. 6. Proposed level scheme for ^{91}Nb. Theoretical positions of levels were calculated on the basis of the shell model

[4]. The transitions between them, 356.6, 819.4 and 2290.7 keV are all coincident. Additionally, the 884.4 and 858.8 keV lines are found to be in coincidence with that prominent cascade. From these results, and in connection with the excitation function, the existence of 4350 keV, and probably 5209 keV levels is suggested. The levels at 1790, 1983.4 and 2033.4 keV were observed by Brown et al. [6]. Our life-time measurements for the level at 1983.4 keV are in agreement with results reported in that paper. The $17/2^-$ level has a long life-time, which is incompatible with [5]. The $15/2^-$ level at 2660 keV was included in the scheme on the basis of angular distribution measurements for transitions with energies 449.4 and 626.4 keV. The levels at 1186.2, 1311, 1581, 1613 and 1637 keV were observed in a (p, γ) experiment [2]. Our angular distribution, as well as excitation function measurements, agree well with the spin values proposed in the mentioned papers. In the single spectrum one can see high energy lines at 2120, 2170, 2330 and 2413 keV. Using angular distributions, excitation functions and coincidence measurements, levels with such energies can be deduced. It follows that these are transitions to the ground state. We have established, by our coincidence measurements, the existence of levels at 2439 and 2902 keV.

4. *Shell model analysis of the experimental results*

The structure of ^{91}Nb can be described by the shell model with ^{88}Sr as an inert core and valence protons restricted to the $2p_{1/2}$ and $1g_{9/2}$ single-particle levels. Such an assumption was made in several theoretical works [7–9, 14]. Taking into account only $(g_{9/2})^3$ and $p_{1/2}(g_{9/2})^2$ configurations means dealing with positive parity ($3/2^+$ to $21/2^+$ with the exception of $19/2^+$) and negative parity ($1/2^-$ to $17/2^-$) levels, respectively. For every theoretically predicted level of $p_{1/2}(g_{9/2})^2$ configurations, we can find its experimental equivalent among our observed levels. Having accepted such a correspondence (the longer lines for the calculated levels in Fig. 6), one is able to evaluate the differences between the two-body matrix elements $V_J - V_0$, where $V_J = \langle (g_{9/2})^2 J | V_{\text{eff}} | (g_{9/2})^2 J \rangle$.

The positions of the negative parity states in ^{91}Nb can be quite easily calculated with the help of Eq. (2) given by Talmi in [15]. All of these are due to $p_{1/2}(g_{9/2})^2$ configurations. The interaction energy in such configurations is diagonal in the scheme in which the $(g_{9/2})^2$ configuration occurs in a definite state (with spin $J = 0, 2, 4, 6, 8$). Thus the eigenstates are characterized by the total spin I and by the spin J. An expression for the difference between the total energy and the energy of the inert core for any such state has the form [15]

$$E_I = C_p + 2C_g + V((g_{9/2})^2 J) + 2\alpha \begin{cases} +\beta J & \text{for } I = J + \frac{1}{2} \\ -\beta(J+1) & \text{for } I = J - \frac{1}{2} \end{cases} \tag{2}$$

where C_p and C_g are single particle energies, α is the mean interaction energy between protons with $p_{1/2}$ and $g_{9/2}$ and equals

$$\alpha = \tfrac{1}{20}\left[9V(p_{1/2}g_{9/2}4) + 11V(p_{1/2}g_{9/2}5)\right] \tag{3}$$

and β is the splitting parameter. For any J value there are two levels with $I = J \pm 1/2$ with energy difference equal to $(2J+1)\beta$. Using Eq. (2) four equations of the type

$$(E_{J+1/2}-E_{1/2^-})+(E_{J-1/2}-E_{J+1/2})\frac{J}{2J+1} = V_J - V_0 \tag{4}$$

are obtained. On inserting experimental energy level values, one obtains in MeV:

$$V_2 = 1.132+V_0, \quad V_4 = 1.832+V_0, \quad V_6 = 2.077+V_0, \quad V_8 = 2.224+V_0. \tag{5}$$

On the other hand, one is able to verify the deteımined quantities using them as parameter values for calculating energy differences between the positive parity states belonging to the $(g_{9/2})^3$ configuration. To perform such a calculation, Eq. (26.37), taken from [16], was used. Taking into account only the diagonal matrix elements of the type

$$\langle (g_{9/2})^3 \alpha JM | \sum_{i<k}^{3} g_{ik} | (g_{9/2})^3 \alpha' JM \rangle \tag{6}$$

and assuming that the interaction conserves seniority, one obtains the energy differences between the positions of the positive parity states. By attributing the experimentai value of 2291 keV to the $13/2^+$ state, one obtains energy positions of the remaining positive parity states. Their values agıee very well with the experimentally observed level values. For example, the probable $(15/2^+)$ state lies lower than the $17/2^+$ state. The energy of the $(11/2^+)$ state, observed for the first time in ouı experiment is in agreement with the theoretical value. The $5/2^+$ level at 1965 keV observed in [2] also appears in our calculations.

It seems that the values proposed for the set of the two-body matrix elements can be used in other theoretical calculations. Similar measurements and calculations for other nuclei of the $g_{9/2}$ region are in progress.

REFERENCES

[1] J. L. Horton, C. L. Hollas, P. J. Riley, S. A. A. Zaidi, C. M. Jones, J. L. C. Ford, Jr., *Nucl. Phys.* **A190**, 362 (1972).
[2] F. Rauch, *Z. Phys.* **243**, 105 (1971).
[3] U. Jahnke, E. Finckh, P. Pietrzyk, B. Schreber, A. Weidinger, Preprint, Hahn-Meitner-Institut für Kernforschung, Berlin.
[4] M. Grecescu, A. Nillsson, L. Harms-Ringdahl, *Nucl. Phys.* **A212**, 429 (1973).
[5] C. V. K. Baba, D. B. Fossan, T. Faestermann, F. Feilitzsch, M. R. Maier, P. Raghavan, R. S. Raghavan, C. Signorini, *Contrib. Int. Conf. Nuclear Moments and Nuclear Structure*, Osaka, Japan, p. 260 (1972).
[6] B. A. Brown, P. M. Lesser, D. B. Fossan, *Phys. Rev. Lett.* **34**, 161 (1975).
[7] N. Auerbach, I. Talmi, *Nucl. Phys.* **64**, 458 (1965).
[8] J. B. Ball, J. B. McGrory, J. S. Larsen, *Phys. Lett.* **41B**, 581 (1972).
[9] D. H. Gloeckner, F. J. D. Serduke, *Nucl. Phys.* **A220**, 477 (1974).
[10] T. Yamazaki, *Nuclear Data* **A3**, 1 (1967).
[11] H. Ejiri, T. Shibata, A. Shimizu, K. Yagi, *J. Phys. Soc. Jap.* **33**, 1515 (1972).
[12] T. Shibata, T. Itahasi, T. Wakatsuki, *Nucl. Phys.* **A237**, 382 (1975).
[13] Nuclear Data Sheets for $A = 91$ prepared by H. Verheul and W. B. Ewbank.
[14] J. Vervier, *Nucl. Phys.* **75**, 17 (1966).
[15] I. Talmi, *Phys. Rev.* **126**, 2110 (1962).
[16] A. de Shalit, I. Talmi, *Nuclear Shell Theory*, Academic Press 1963.